Current feedback operational amplifiers as fast charge sensitive preamplifiers for photomultiplier read out

2011 JINST 6 P05004

(http://iopscience.iop.org/1748-0221/6/05/P05004)

PUBLISHED BY IOP PUBLISHING FOR SISSA

RECEIVED: *October 25, 2010*
REVISED: *April 8, 2011*
ACCEPTED: *May 2, 2011*
PUBLISHED: *May 9, 2011*

Current feedback operational amplifiers as fast charge sensitive preamplifiers for photomultiplier read out

A. Giachero,[a,b] **C. Gotti,**[a,c,1] **M. Maino**[a,b] **and G. Pessina**[a,b]

[a] *INFN — Sezione di Milano-Bicocca, I-20126, Milano, Italy*
[b] *Dip. di Fisica, Università degli Studi di Milano-Bicocca, I-20126, Milano, Italy*
[c] *Dip. Elettronica e TLC, Università degli Studi di Firenze, I-50139, Firenze, Italy*

E-mail: claudio.gotti@mib.infn.it

ABSTRACT: Fast charge sensitive preamplifiers were built using commercial current feedback operational amplifiers for fast read out of charge pulses from a photomultiplier tube. Current feedback opamps prove to be particularly well suited for this application where the charge from the detector is large, of the order of one million electrons, and high timing resolution is required. A proper circuit arrangement allows very fast signals, with rise times down to one nanosecond, while keeping the amplifier stable. After a review of current feedback circuit topology and stability constraints, we provide a ”recipe” to build stable and very fast charge sensitive preamplifiers from any current feedback opamp by adding just a few external components. The noise performance of the circuit topology has been evaluated and is reported in terms of equivalent noise charge.

KEYWORDS: Analogue electronic circuits; Front-end electronics for detector readout

[1] Corresponding author.

doi:10.1088/1748-0221/6/05/P05004

2011 JINST 6 P05004

Contents

2011 JINST 6 P05004

1 Introduction to current feedback opamps (CFOAs)

When dealing with high frequency applications requiring bandwidth above the hundred MHz range, most voltage feedback operational amplifiers (VFOAs) cannot be used. This is simply because their maximum bandwidth is often below this frequency range. Even the fastest VFOAs which can reach these frequencies at unity gain are not useful because the requirement of gain reduces the available bandwidth due to the well-known "gain-bandwidth product" tradeoff. Under compensated opamps are another option, but the amplifier bandwidth and stability turn out to be highly dependent on the detector capacitance. Thus it is difficult to use commercial VFOAs in building fast charge sensitive preamplifiers because both gain and high bandwidths are usually required.

In recent years, current feedback operational amplifiers (CFOAs) have been introduced. This opamp topology allows for a wide bandwidth, absence of slew rate limitation, and above all, essentially the absence of a gain-bandwidth product limit. This occurs because the bandwidth of the current feedback topology, in a first order analysis, is independent of gain and only depends on the value of the feedback resistor. Thus CFOAs allow any amplification factor without the corresponding bandwidth narrowing of a traditional VFOA. The tradeoff is that CFOAs have poor DC precision and require more effort to achieve closed loop stability. For a broader introduction on current feedback operational amplifiers, we refer to [1–4].

Figure 1 shows the simplified model of a CFOA. The non-inverting input has high impedance, as with VFOAs, and its voltage is buffered to the inverting input, forcing a zero voltage difference between the two. The inverting input is thus a low impedance node (unlike the inverting input of a VFOA) whose impedance we denote by R_{ib}. The current i_n flowing out of the inverting input

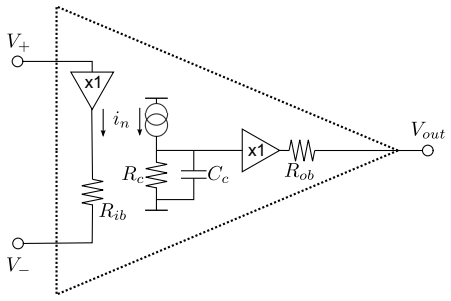

Figure 1. Simplified equivalent schematic of an ideal CFOA, with a dominant pole only.

is mirrored to an internal high impedance node, formed by the parallel network of resistor R_c and capacitor C_c, where it is converted to a voltage. A unity gain buffer with a low output impedance $R_{\rm ob}$ brings this voltage to the output. By converting the outgoing current at the inverting input to a voltage at the output, this makes the CFOA a transimpedance device. In the frequency domain, and by neglecting the small voltage drop due to $R_{\rm ob}$, we have

$$V_{\rm out}(s) = \frac{R_c}{1+sR_cC_c} i_n(s) \equiv Z_{\rm OL}(s)\, i_n(s). \tag{1.1}$$

From a general point of view, in real CFOAs, i_n can be mirrored by an $m:1$ ratio, i.e. with a multiplicative factor. With this, a gain can be set at the output stage, which again we can indicate by m; in any of these cases, the factor m should be included in equation 1.1. However, $Z_{\rm OL}$ can be redefined to absorb it. To keep our model as simple as possible, we will consider in the following that this is the case, even though it will mask the real values of R_c and C_c with new effective values $R_c' \equiv mR_c$, $C_c' \equiv C_c/m$, with $Z_{\rm OL}$ containing these new values instead of the real ones. Typical values are about 100 kΩ for R_c and about 1 pF for C_c, varying between different CFOAs.

So far we have investigated the open loop configuration with no feedback from the output to the input. The open loop transimpedance $Z_{\rm OL}$ is very high at DC, where R_c dominates, and rolls off with increasing frequency at a 20 dBΩ/dec because of the dominant pole at frequency $1/2\pi C_cR_c$. This is exactly like the open loop gain of a VFOA, aside from the fact that the units are in impedance. In equation 1.1, as well as in 1, the additional high frequency poles of $Z_{\rm OL}$ have been neglected. However, their contribution ultimately determines the maximum bandwidth of the CFOA and they can be accounted for by including a multiplicative factor in $Z_{\rm OL}$:

$$Z_{\rm OL}(s) \equiv \frac{R_c}{1+sR_cC_c} G(s), \tag{1.2}$$

where

$$G(s) \equiv \frac{1}{1+s\tau_1}\frac{1}{1+s\tau_2}\ldots \tag{1.3}$$

and τ_i are the time constants associated with the additional poles in $Z_{\rm OL}$. The number of additional poles is not a critical issue, since a single pole is usually enough to allow a complete understanding of the frequency response of a real CFOA. For an ideal CFOA, all τ_i are equal to zero and $G \equiv 1$. The open loop transimpedance $Z_{\rm OL}$ of a typical CFOA with a low frequency dominant pole and high frequency additional poles is depicted in figure 2.

2011 JINST 6 P05004

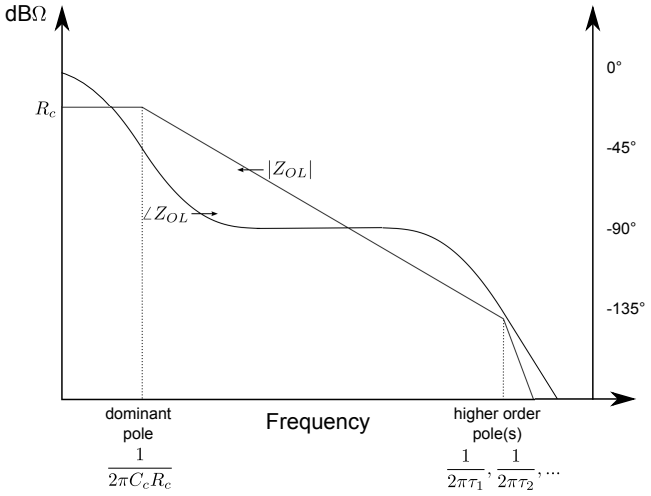

Figure 2. Magnitude and phase of the open loop transimpedance of a typical CFOA, with a low frequency dominant pole and high frequency additional poles.

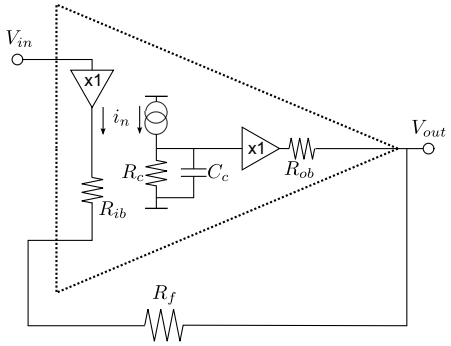

Figure 3. The CFOA buffer: schematic.

The fact that the output has the same sign of the current i_n, as can be seen from equation 1.1, allows application of negative feedback as is commonly done for VFOAs. By putting a resistor from the output to the input, one obtains the closed loop structure depicted in figure 3. In this circuit the small resistances $R_{\rm ib}$ and $R_{\rm ob}$ can be neglected, because they have very small values and are in series with R_f. This circuit is a voltage follower, i.e. a buffer, and is the same as the VFOA configuration. However, contrasting with the VFOA case, the output cannot be shorted to the inverting input. For CFOAs to be stable, a minimum value of resistive feedback is always required. If the value of R_f in figure 3 is less than a minimum value (usually around a few hundred Ohms depending on the specific CFOA), the CFOA will oscillate. To understand why this happens, a bit of insight on the exact behavior of the feedback structure is necessary and is the subject of the next section.

2 Loop gain calculation in the current feedback topology

As common practice in the study of operational amplifier circuits and feedback structures in general, the loop gain plays a crucial role (see for instance [5]).

2011 JINST 6 P05004

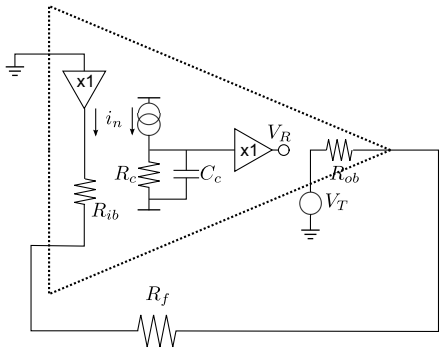

Figure 4. The CFOA buffer: loop gain calculation.

The loop gain is defined as the gain of a signal injected at any node of the feedback loop resulting from traveling all the way around the loop and back to the starting node. In the case of operational ampliers, the easiest way to calculate the loop gain is to break the loop at the output of the opamp and null the input sources, as depicted in figure 4 for the CFOA buffer. By injecting the test signal V_T, we can calculate the voltage V_R generated at the output of the opamp. The loop gain is the ratio $T = V_R/V_T$. Since the circuit is linear,[1] T does not depend on V_T. Ideally, the test signal V_T should be injected before $R_{\rm ob}$. Here $R_{\rm ib}$ and $R_{\rm ob}$ are depicted for completeness, but their value is very low, usually tens of Ohms, and they affect signal and loop gain expressions only marginally. Their contribution can be neglected for the moment.

In the case of the CFOA buffer, the loop gain is

$$T(s) = -\frac{Z_{\rm OL}(s)}{R_f}. \tag{2.1}$$

This is true even if the CFOA buffer is modified by adding a resistor R_n between the inverting input and ground. In this case, it can be shown that the gain becomes $1 + R_f/R_n$, the same as with a VFOA, but the loop gain is still given by 2.1. Thus for CFOAs, as long as the effects of $R_{\rm ib}$ and $R_{\rm ob}$ can be neglected, the loop gain is decoupled from the signal gain and depends only on the value of the feedback resistor.

Every CFOA is optimized for a specific R_f value, which we denote by R_f^*, to be found in the datasheet. Since $Z_{\rm OL}$ has a dominant pole, which gives a -90 degrees phase shift, and then additional poles at higher frequency, which drive its phase to -180 degrees, R_f^* is simply the value large enough to make $|T| = 1$ well before $Z_{\rm OL}$ reaches a -180 degrees phase shift, i.e. before $s \gg \tau_1^{-1}$. At high frequency, when $s \gg \tau_1^{-1}$, the -180 degrees phase shift cancels the minus sign in 2.1 and the negative gain of the feedback loop becomes positive. When this happens, if $|T| > 1$ the input is forced to larger and larger values and leads to instability in the feedback loop. On the other side, if $|T| < 1$ then stability is preserved. Conventionally, a feedback network is considered stable if the phase of T in $|T| = 1$, called the "phase margin", is larger than 45 degrees. This is shown in figure 5, where the magnitude of $Z_{\rm OL}$ and R_f are plotted (so that $|T| = 1$ occurs at the crossing between the curves) as well as the phase of T, from which the phase margin can be read. If a smaller value is

[1] Consider a circuit driven by a voltage source $V_{\rm in}$. Let us denote its output by $V_{\rm out}(V_{\rm in})$. A circuit is called linear if $V_{\rm out}(aV_{\rm in}) = aV_{\rm out}(V_{\rm in})$, where a is a real number.

2011 JINST 6 P05004

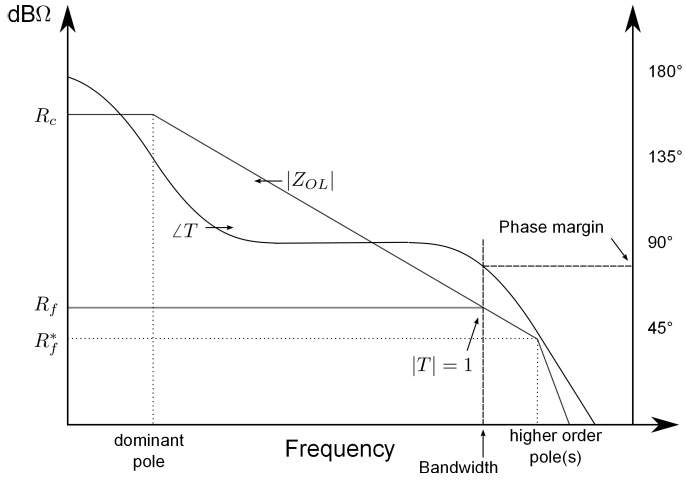

Figure 5. The CFOA buffer: loop gain Bode plot. Plotting the magnitude of Z_{OL} and R_f and phase of T versus frequency helps to visualize feedback stability issues.

used for R_f, the condition $|T| = 1$ is pushed to higher frequency which increases the bandwidth but leads to instability. This is because the phase margin becomes less than 45 degrees. On the other side, a higher value for R_f causes the loop gain to roll off earlier to $|T| = 1$, trading bandwidth for a larger phase margin. Instead of the constant "gain-bandwidth" product in VFOAs, one can think of CFOAs as having a constant "feedback resistor-bandwidth" product.

Despite the differences, it still holds for CFOAs that the voltage at the inverting input follows the non-inverting, and that current entering the opamp inputs is nearly zero. Thus a CFOA can be used in any VFOA configuration, with full bandwidth at nearly any gain, provided that the additional constraints on the feedback path needed for stability are met. A quick review of many CFOA circuits can be found in [6]. From a general point of view, the feedback path can also contain inductors or capacitors. In this case, in the loop gain calculations it is only necessary to replace the feedback resistance R_f with the complex feedback impedance $Z_f(s)$, to take into account the inductive or capacitive contributions. Z_f is defined as the conversion factor from the test voltage V_T to the current entering the inverting node of the CFOA, i.e. $Z_f(s) \equiv (-i_n(s)/V_T)^{-1}$, which again will not depend on V_T. The Bode plot of Z_{OL} and Z_f is a very useful tool to determine the phase of T when $|T| = 1$. The case of capacitive feedback, required by charge sensitive preamplifiers, is addressed in the next section.

3 Capacitive feedback and CFOAs

When dealing with applications that require a capacitor C_f in the feedback loop of a CFOA, such as charge preamplifiers, particular care must be taken to keep the circuit stable. The simplest opamp based charge preamplifier (or current integrator) is depicted in figure 6, where the feedback path is the parallel network of a resistor and a capacitor. The capacitor integrates the current at the negative input, while the resistor (whose value is usually large) discharges it slowly after each pulse for DC restoration. The current generator models the charge pulse from the detector, whose capacitance is

2011 JINST 6 P05004

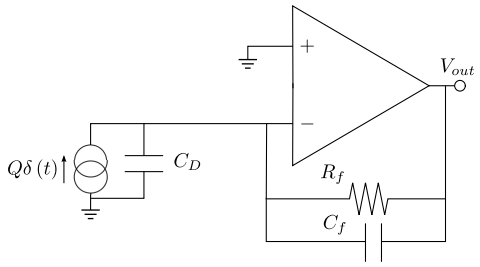

Figure 6. The classic opamp-based charge sensitive preamplifier circuit.

C_D. With a VFOA, the loop gain is

$$T_{\mathrm{VF}}(s) = -A(s)\frac{1+sC_fR_f}{1+s(C_D+C_f)R_f}, \tag{3.1}$$

where $A(s)$ is the open loop gain of the opamp. Here no stability problems arise as long as the VFOA is unity gain stable, or at least stable at a gain equal to $(C_D+C_f)/C_f$.

On the other side, if a CFOA is used in this configuration, the loop gain is (again assuming R_{ib} and R_{ob} to be negligible)

$$T(s) = -\frac{Z_{\mathrm{OL}}(s)}{Z_f(s)} = -Z_{\mathrm{OL}}(s)\frac{1+sR_fC_f}{R_f} \simeq -sC_fZ_{\mathrm{OL}}(s), \tag{3.2}$$

where the last approximation is valid if R_f is large. Thus for the CFOA the pole due to C_D in equation 3.1 is missing. As a consequence, T does not roll off with the dominant pole in Z_{OL}, since the zero due to C_f cancels it out. T begins to roll off only when it reaches the second pole in Z_{OL}, given by τ_1. But then other poles $(\tau_2, \ldots)$ occur before $|T| = 1$, leading to oscillation. The Bode plot for this case is shown in figure 7: as can be seen, there is no phase margin, thus the system will be unstable. This is the reason why designers often avoid capacitive feedback with CFOA applications, and must circumvent the problem with additional constraints or different circuit configurations (see, for example, [7, 8]).

4 The CFOA as a charge sensitive preamplifier

The known stability problem of the CFOA with capacitive feedback at first sight appears to be daunting when considering the possibility of using a CFOA to build a charge sensitive preamplifier. Fortunately there is a way to exploit the open loop characteristics of a CFOA and circumvent the problem. It does not allow the same flexibility as the classic VFOA configuration, as will be discussed, but it can be a very useful way to build a fast charge preamplifier when low power dissipation, low noise and high gain are not mandatory. This can be useful for instance when evaluating the timing characteristics of photomultipliers without a dedicated read out chain.

We should first notice that the open loop CFOA is a current transimpedance integrator. When the non-inverting input is grounded, the current entering the inverting input is multiplied by the open loop transimpedance Z_{OL}. If the incoming pulse of charge Q from the detector at $t = 0$ is given by $I_{\mathrm{in}}(t) = Q\delta(t)$, or, in the complex frequency domain, $I_{\mathrm{in}}(s) = Q$, then the open loop

2011 JINST 6 P05004

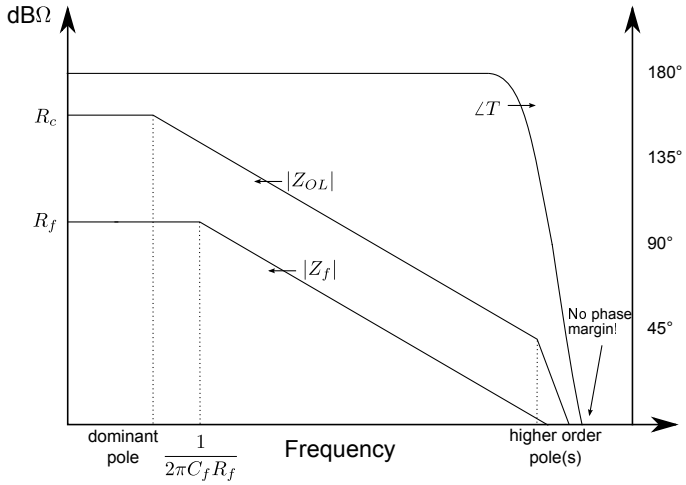

Figure 7. The classic opamp charge sensitive preamplifier: loop gain Bode plot, showing that this configuration will not work with a CFOA.

CFOA gives an output signal

$$V_{\text{out}}(s) = -Z_{\text{OL}}(s) I_{\text{in}}(s) = -Q \frac{R_c}{1 + sR_cC_c} G(s)\,. \tag{4.1}$$

Putting $G(s) = 1$ as for an ideal CFOA, in the time domain, the preceding expression becomes

$$V_{\text{out}}(t) = -\frac{Q}{C_c} \exp\left(-\frac{t}{R_cC_c}\right) \theta(t)\,, \tag{4.2}$$

where $\theta(t)$ is the ideal step function, which equals 0 if $t < 0$ and 1 otherwise. This signal is a pulse with zero rise time, instantaneously peaking at a voltage $-Q/C_c$, then slowly discharging with time constant R_cC_c. With typical values of $R_c = 100$ kΩ, $C_c = 1$ pF, the peak amplitude would be 160 mV/Me$^-$ and the discharge time constant $\tau_f = 100$ ns. Since the fall is exponential, the 90% to 10% fall time is given by $2.2\tau_f$, or 220 ns with the values above. Figure 8 shows the response of a Texas Instruments OPA695 to a 1 Me$^-$ charge injected at the inverting input. Note that the measurement was taken at the far end of a 50 Ω terminated cable, so the measured signal amplitude is halved. The values estimated from figure 8 are about $C_c = 1$ pF (from the peak amplitude) and $R_c = 70$ kΩ (from the fall time). These values are in rough agreement with those obtained directly from the plot of Z_{OL} in the OPA695 datasheet. It should be noted that C_c and R_c suffer from the inherent lack of precision of integrated resistors and capacitors, which can reach a process spread of about 30%, whereas discrete passive components are available with much higher precision.

This open loop configuration yields the maximum gain and the fall time achievable with a particular CFOA in the configuration to be described in the following. A very large feedback resistor can be used to achieve this condition while stabilizing the DC working point. Incidentally, the OPA695 was found to work even without any feedback resistor, i.e. open loop at DC, but this is an exception among CFOAs.

Gain and fall time of the open loop configuration can be modified with the circuit shown in figure 9. As will be clear after the calculations, the purpose of the feedback resistor R_f is to shorten

2011 JINST 6 P05004

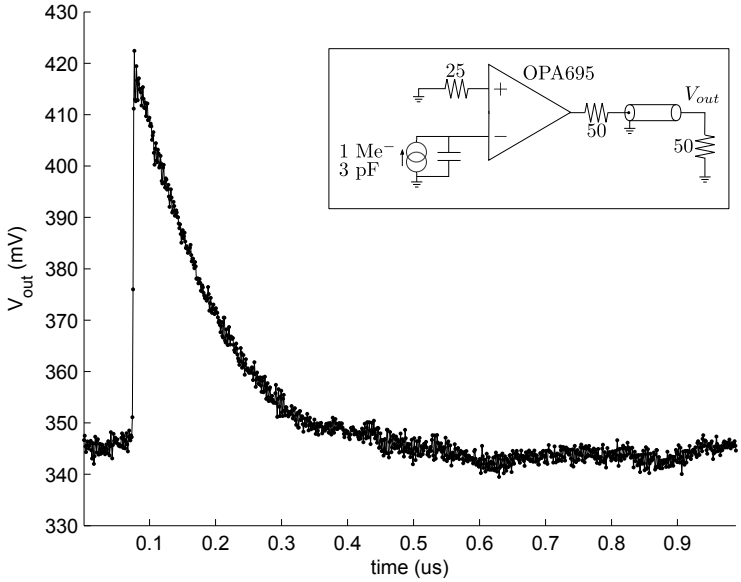

Figure 8. Voltage pulse from an open loop OPA695 from Texas Instruments with a 1 Me^- charge at the input. The inlay shows the schematic.

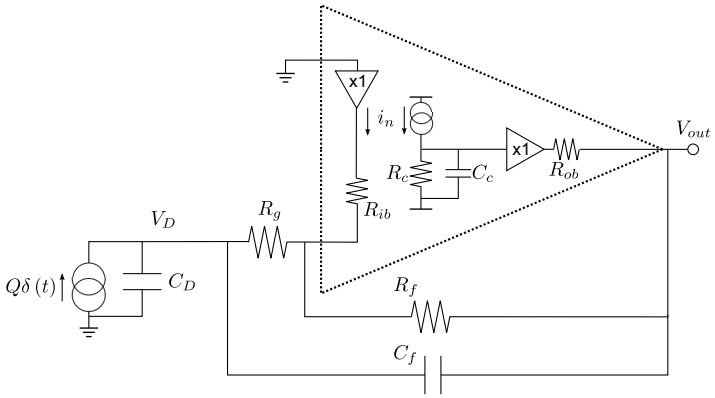

Figure 9. The CFOA as a charge sensitive preamplifier.

the fall time with respect to the open loop value, and does not affect gain nor stability as long as $R_f \gg R_f^*$. The purpose of the feedback capacitor C_f is to decrease gain if necessary. In order to keep this configuration stable, the resistor R_g was put in series with the CFOA input.

First of all, let us consider the stability of this configuration. By calculating the loop gain T from figure 10, neglecting $R_{\rm ib}$ and $R_{\rm ob}$, we obtain

$$T(s) = \frac{V_R}{V_T} = -\frac{Z_{\rm OL}(s)}{Z_f(s)} = -\frac{Z_{\rm OL}(s)}{R_f}\left(\frac{1+s\left[C_f R_f + (C_D+C_f)R_g\right]}{1+s(C_D+C_f)R_g}\right). \tag{4.3}$$

The corresponding Bode plot is depicted in figure 11. This expression makes clear the role of R_g to guarantee stability, providing a zero in Z_f to compensate the pole at high frequency. As was pointed out in the introduction, feedback is stable as long as $|T| < 1$ when $Z_{\rm OL}$ reaches its higher

2011 JINST 6 P05004

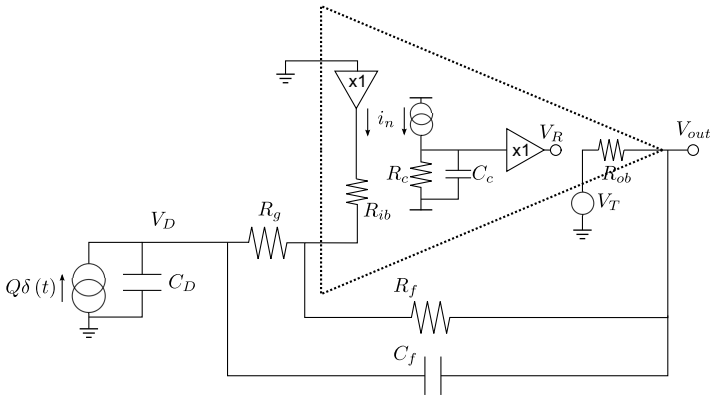

Figure 10. The CFOA as a charge sensitive preamplifier: circuit diagram for loop gain calculation.

order poles. Since $Z_{\rm OL} \simeq R_f^*$ at the frequency of the higher order poles, the stability condition is a constraint on the minimum value of the feedback impedance Z_f at high frequency. In our case, from equation 4.3, we have that at high frequency the value of the feedback impedance is

$$Z_f \simeq \frac{(C_D + C_f) R_g R_f}{(C_D + C_f) R_g + C_f R_f}, \tag{4.4}$$

which must be larger than R_f^* for stability. Since as we shall see all the other parameters are usually set by the application requirements, the stability condition becomes a constraint on the minimum value of R_g:

$$R_g > \frac{C_f}{C_D + C_f} \frac{R_f R_f^*}{R_f - R_f^*} \equiv \frac{C_f}{C_D + C_f} R_x. \tag{4.5}$$

where R_x is defined as the resistance value such that if is put in parallel with a resistor of value R_f, gives an equivalent resistance R_f^*, i.e. $R_x || R_f \equiv R_f^*$. Assuming R_f to be much larger than R_f^*, we can approximate $R_x \simeq R_f^*$, and equation 4.5 becomes

$$R_g > \frac{C_f}{C_D + C_f} R_f^*, \tag{4.6}$$

regardless of the value of R_f.

Let us now calculate the gain expression. From figure 9, we have the node equations

$$-Q + sC_D V_D + sC_f (V_D - V_{\rm out}) + \frac{V_D}{R_g} = 0 \tag{4.7}$$

at the detector node, and

$$\frac{V_D}{R_g} + \frac{V_{\rm out}}{R_F} + \frac{V_{\rm out}}{Z_{\rm OL}(s)} = 0 \tag{4.8}$$

at the CFOA input node, where equation 1.1 was used to turn the current i_n at the inverting node into the last part of the sum. Solving the system for $V_{\rm out}$ gives

$$V_{\rm out}(s) = -\frac{R_f || Z_{\rm OL}(s)}{1 + s\Big(C_f \left(R_f || Z_{\rm OL}(s)\right) + (C_D + C_f) R_g\Big)} Q. \tag{4.9}$$

2011 JINST 6 P05004

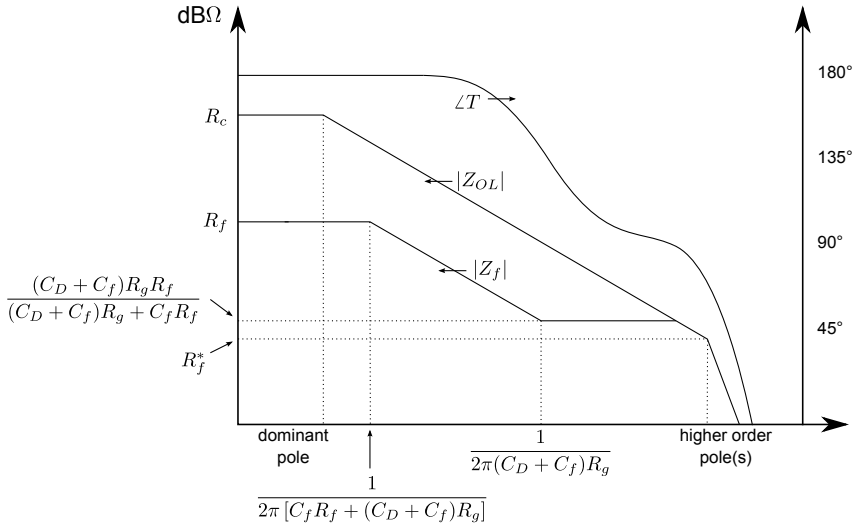

Figure 11. The CFOA as a charge sensitive preamplifier: loop gain Bode plot.

Here R_g gives a negligible contribution, as long as its value is kept at the minimum allowed by equation 4.6, i.e. if $R_g = R_f^* C_f/(C_D+C_f)$. Then equation 4.9 becomes

$$V_{\text{out}}(s) = -\frac{R_f||Z_{\text{OL}}(s)}{1+sC_f\left(R_f||Z_{\text{OL}}(s)+R_f^*\right)}Q, \tag{4.10}$$

which, if $R_f \gg R_f^*$, and substituting equation 1.2 for $Z_{\text{OL}}(s)$, becomes

$$V_{\text{out}}(s) = -\frac{R_fR_cG(s)}{R_f+R_cG(s)+sR_fR_c\left(C_fG(s)+C_c\right)}Q. \tag{4.11}$$

Now if we assume that $R_c \gg R_f$, and thus let $R_c \to \infty$ (otherwise the parallel $R_f||R_c$ should be considered in the following equations in place of R_f alone) we obtain

$$V_{\text{out}}(s) = -\frac{R_f}{1+sR_f\left(C_f+C_c/G(s)\right)}Q. \tag{4.12}$$

Finally, if we set $G(s)=1$, neglecting the high frequency poles of the CFOA, we have

$$V_{\text{out}}(s) = -\frac{R_f}{1+sR_f\left(C_f+C_c\right)}Q, \tag{4.13}$$

which in time domain becomes

$$V_{\text{out}}(t) = -\frac{Q}{C_f+C_c}\exp\left(-\frac{t}{R_f(C_f+C_c)}\right)\theta(t). \tag{4.14}$$

This expression is just like the open loop response of equation 4.2, but with a gain given by C_f+C_c, and a fall time which is determined by R_f instead of R_c.

Neglecting $G(s)$, as in equation 4.13, means to assume that the CFOA is ideal, without any bandwidth limitation. This leads to a zero rise time in equation 4.14. When a first order contribution

2011 JINST 6 P05004

from $G(s)$ is taken into account, so that one high frequency pole from equation 1.3 is introduced in equation 4.12, then the frequency response becomes

$$V_{\text{out}}(s) = -\frac{R_f}{1+sR_f(C_f+C_c)+s^2R_fC_c\tau_1}Q. \tag{4.15}$$

The denominator now has two poles very far from each other. One is approximately located at

$$p' = \frac{1}{R_f(C_c+C_f)}, \tag{4.16}$$

as for the ideal case given in equation 4.13, while the other is located at higher frequency:

$$p'' = \frac{C_f+C_c}{C_c\tau_1}. \tag{4.17}$$

The higher frequency pole gives the time constant associated with the rise time of the output pulse, which is basically τ_1. Equation 4.17 suggests that the rise time could be lowered by increasing C_f. However, higher order poles (τ_2, ...) have been neglected in that calculation, as well as the slew rate limitations of the CFOA, so the time constant can hardly be less than τ_1 in any case. Since the rise is exponential, the 10% to 90% rise time is given by $2.2\tau_1$.

The value of τ_1 can be estimated from the open loop transimpedance plot or from the maximum bandwidth of the CFOA, both to be found in the datasheet. An important fact should be pointed out here: when manufacturers claim in a CFOA datasheet that the bandwidth exceeds 1 GHz, they often mean that such a speed can be achieved in the buffer configuration via a small phase margin, i.e. via a controlled amount of peaking in the frequency response. The second pole of the CFOA is often located one or two octaves lower, as can be seen from the position of the higher order poles in the plot of the open loop transimpedance. We observed this in many commercial CFOAs, whose high order poles sit around 400 MHz, but can be used in buffer configuration up to 1 GHz and above by reducing the phase margin to less than 30 degrees. If the second pole is located at $f_1 = 400$ MHz, then $\tau_1 \simeq 0.4\,ns$, and so the rise time in response to the charge pulse turns out to be about 1 ns.

So far we have neglected the output impedances of the input and output buffers, which we denoted by R_{ib} and R_{ob} respectively. Their values are very small, however they can have an impact on stability. By equation 4.5, if C_f is not used, then there is no need for R_g. This is not true anymore if the effect of R_{ib} is considered. If the detector capacitance C_D is large enough, then an additional pole in T can occur at frequency $1/2\pi R_{\text{ib}}C_D$. This leads to additional phase shift and instability in the feedback loop unless R_f is large enough to let this additional pole fall out of the bandwidth of the amplifier. A small R_g can compensate this pole: in this case the loop gain with $C_f = 0$ is approximately given by

$$T(s) = -\frac{Z_{\text{OL}}(s)}{R_f}\frac{1+sC_DR_g}{1+sC_D(R_g+R_{\text{ib}})}. \tag{4.18}$$

It is clear from this expression that even when C_f is zero a small R_g of about 25 to 50 Ω should be used to assure the stability of the system.

A similar effect can be produced by R_{ob} and the series combination of C_f and C_D by introducing a pole at the output with feedback taken via R_f. The calculations in this case, neglecting R_{ib},

2011 JINST 6 P05004

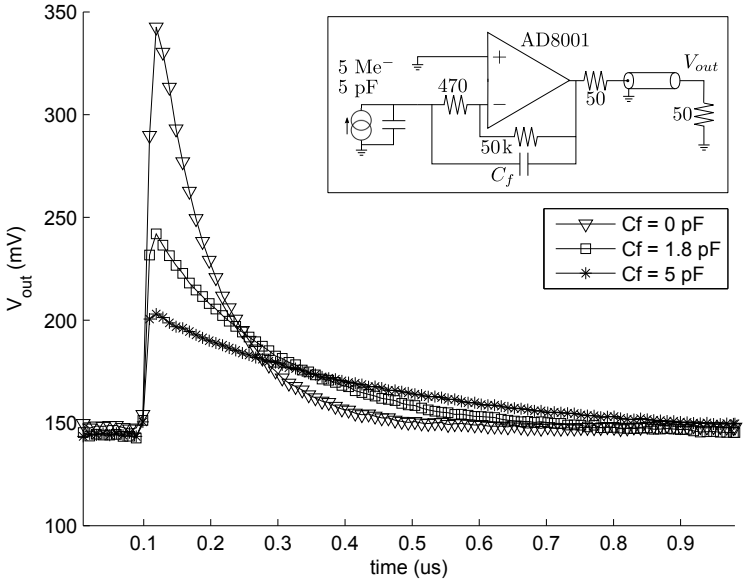

Figure 12. Voltage pulses from an AD8001 from Analog with a 5 Me^- charge at the input, with different values of feedback capacitance C_f.

give the approximate result (for $R_{\rm ob} \ll R_g, R_f$)

$$T(s) = -\frac{Z_{\rm OL}(s)}{R_f}\frac{1+s\left[C_f R_f + (C_D+C_f)R_g\right]}{1+s(C_D+C_f)R_g + s^2 C_D C_f R_g R_{\rm ob}}. \tag{4.19}$$

This expression shows an additional pole at high frequency, due to $R_{\rm ob}$, which can lead to instability. This problem was observed both in the OPA695 from TI and in the LMH6702 from National, but not in the AD8001 from Analog, which is slightly slower, so that the pole fell out of the bandwidth of the amplifier. To circumvent this problem, a small resistor R_h should be put in series with C_f to decouple the capacitive load from the output of the CFOA and add a zero to compensate the pole. The loop gain, evaluated in the case where $R_h, R_{\rm ob} \ll R_g, R_f$ for conciseness, becomes

$$T(s) = -\frac{Z_{\rm OL}(s)}{R_f}\frac{1+s\left[C_f R_f + (C_D+C_f)R_g\right] + s^2 C_D C_f R_h R_{\rm ob}}{1+s(C_D+C_f)R_g + s^2 C_D C_f (R_g+R_h) R_{\rm ob}}. \tag{4.20}$$

Again a value of about 25 to 50 Ω should be used for R_h.

Figure 12 shows the response of an AD8001 800 MHz CFOA from Analog in response to 5 Me^- charge at the input. The detector capacitance is $C_D = 5$ pF, and the feedback resistors are $R_f = 50$ kΩ, $R_g = 470$ Ω. Three values for C_f were used: 0 pF, showing the effect of C_c alone, then $C_f = 1.8$ pF and $C_f = 5$ pF. From this measurement, a value of about $C_c = 2$ pF can be extracted. Here no resistor R_h in series with C_f was necessary. The rise time was found to be as low as a few nanoseconds, as allowed by the bandwidth of the AD8001.

Figure 13 shows the response of a LMH6702 1.7 GHz CFOA from National in response to charge pulses of 300 ke^-, coming from a detector of capacitance 0.5, 5 or 50 pF. Feedback resistor is $R_f = 5$ kΩ, while R_g was set to 50 Ω to improve stability, even if C_f is not present. From these

2011 JINST 6 P05004

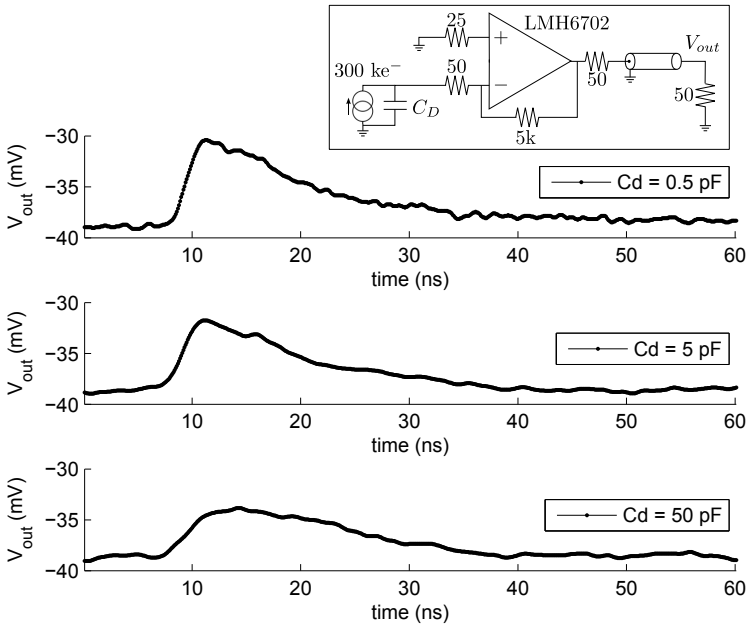

Figure 13. Voltage pulses from a LMH6702 from National with pulses of 300 ke$^-$ charge at the input and different values of detector capacitance.

measurements, a value of C_c of about 3 pF can be estimated. Note that the shape of the signal is almost the same in all three cases; for the upper measurement with low C_D, rise time is limited by the rise time of the pulser that was used (2.5 ns). With increasing C_D, there is a low pass filter effect due to C_D and R_g, limiting rise time to $2.2C_DR_g$ and chopping the peak of the pulse (thus giving the illusion of a lower gain). However this measurement shows that a wide range of detectors with varying capacitances can be read out using this configuration causing only minor changes in the output signal characteristics. In contrast, with the usual VFOA charge sensitive preamplifier, the rise time is roughly proportional to the detector capacitance and it would change by a factor of 100 over this range.

5 The “recipe”

Let us now summarize the steps to be taken when using our approach to build a charge sensitive preamplifier with a commercial CFOA. To begin, one must know the characteristics of the detector to be read out: the charge Q it yields and its capacitance C_D. Note that, as will be calculated in the next section, only charge pulses which exceed about 100 ke$^-$ can be read out with this approach.

5.1 Choosing the CFOA

The position of the poles in Z_{OL} can be estimated from the plot of Z_{OL} given in the datasheet of any CFOA. As an example, we include in this paper the Z_{OL} Bode plot (magnitude and phase) from the datasheet of the Texas Instruments OPA695 CFOA, shown in figure 14. From the frequency f_0 of the dominant pole, where Z_{OL} starts to decrease, and from the DC value of Z_{OL}, which is R_c, one

2011 JINST 6 P05004

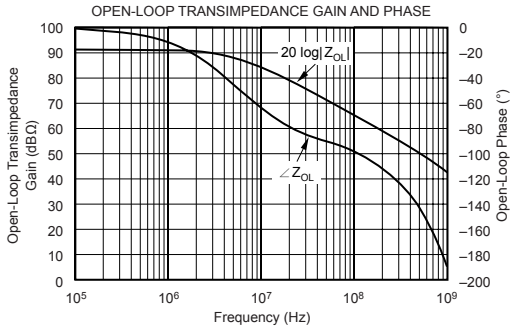

Figure 14. Open loop transimpedance of the OPA695 from TI, taken from the datasheet.

can estimate the value of the internal capacitance C_c as

$$C_c = \frac{1}{2\pi f_0 R_c}. \tag{5.1}$$

In the example of the OPA695, R_c is a bit more than 90 dBΩ, or 40 kΩ. The frequency of the first pole is located at about 4 MHz, so the value of C_c can be estimated to be about 1 pF. The other important piece of information to find in the datasheet is the value of the optimal feedback resistance R_f^*, which is 500 Ω for the OPA695. The value of τ_1, related to the position of the higher order poles, can be estimated by looking at the frequency f_1 where the slope of $Z_{\rm OL}(s)$ doubles, or more easily by looking at the frequency where $|Z_{\rm OL}| = R_f^*$, which happens at

$$f_1 = \frac{1}{2\pi R_f^* C_c}, \tag{5.2}$$

then obtaining the time constant as

$$\tau_1 = \frac{1}{2\pi f_1}. \tag{5.3}$$

The 10% to 90% rise time of the output pulse is given by $t_{\rm rise} = 2.2\tau_1$ (unless limited by the charge collection time in the detector). For the OPA695, the frequency f_1 where $|Z_{\rm OL}| = 500$ Ω is found to be about 500 MHz, τ_1 is 300 ps and $t_{\rm rise} \simeq 700$ ps.

5.2 Gain

Without C_f, the peak value of the output voltage from equation 4.14 is given by

$$V_{\rm peak} = \frac{Q}{C_c}. \tag{5.4}$$

That is about 160 mV/Me$^-$ for the OPA695 with $C_c \simeq 1$ pF. If a higher gain is required, then one should find a CFOA with a smaller C_c, or try a different configuration. For CFOAs commercially available at the time of this writing, C_c can range from about 0.5 pF to 3 pF. If the gain in 5.4 fits the application, then C_f is not necessary. However, relying on C_c alone makes the gain and fall time suffer because of the large production spread of integrated capacitors. A small external C_f can be used to make the gain and fall time more predictable at the price of a gain reduction. The use of an external feedback capacitor C_f decreases the height of the voltage peak to

$$V_{\rm peak} = \frac{Q}{C_c + C_f}. \tag{5.5}$$

2011 JINST 6 P05004

5.3 Fall time

The time constant of the exponential discharge is given by $(C_f + C_c)(R_f||R_c)$. The 90% to 10% fall time of the output pulse is thus given by $t_{\text{fall}} = 2.2(C_f + C_c)(R_f||R_c)$. If R_c is large enough, then the fall time is determined by R_f alone, which can be chosen to give the required fall time:

$$R_f = \frac{t_{\text{fall}}}{2.2(C_f + C_c)}. \tag{5.6}$$

The value for R_f should in any case be bigger than R_f^*, to guarantee stability, and smaller than R_c. If R_f is larger than R_c, then the fall time is set by R_c and the only purpose of R_f is to stabilize the DC working point. This should in any case guarantee enough freedom: in the example of the OPA695, with C_c = 1 pF, R_c = 40 kΩ, R_f^* = 500 Ω, assuming $C_f = 0$, R_f can range from about 1 kΩ, which yields a 3 ns fall time, to infinity, which yields about 100 ns fall time since in this case the discharge is on R_c alone, as in the open loop case.

5.4 Stability

After setting C_f and R_f, one should choose R_g from equation 4.6 to guarantee stability:

$$R_g = \frac{C_f}{C_D + C_f} R_x, \tag{5.7}$$

where C_D is the detector capacitance and

$$R_x \equiv \frac{R_f R_f^*}{R_f - R_f^*}. \tag{5.8}$$

Even if C_f is not used, a small R_g of about 25 to 50 Ω should be used, at least with the fastest CFOAs, to compensate the pole given by C_D with the input buffer output resistance R_{ib}. Also a small R_h of about the same value should be put in series with C_f to compensate the pole due to direct capacitive load at the output of the CFOA.

6 Noise performance and equivalent noise charge

Let us now suppose there is a shaping filter after the preamplifier, a common practice in detector read out to improve the noise performance of the read out chain. The shaper makes it necessary in our calculations to convert the noise sources of the preamplifier, which are expressed in terms of power spectra, to the so-called ”equivalent noise charge” (ENC). ENC is the amount of charge from the detector for which the signal equals the noise and below which no charge pulse can be detected [9, 10].

For the sake of simplicity, let us assume the shaping filter to be of the simple CR-RC type, with time constant τ, thus giving a transfer function

$$F(s) = \frac{s\tau}{(1 + s\tau)^2}, \tag{6.1}$$

where τ has to be smaller than the preamplifier discharge constant $(C_f + C_c)(R_f||R_c)$, and larger than the higher order zero of Z_f at frequency $1/2\pi R_g(C_D + C_f)$. These conditions guarantee that

2011 JINST 6 P05004

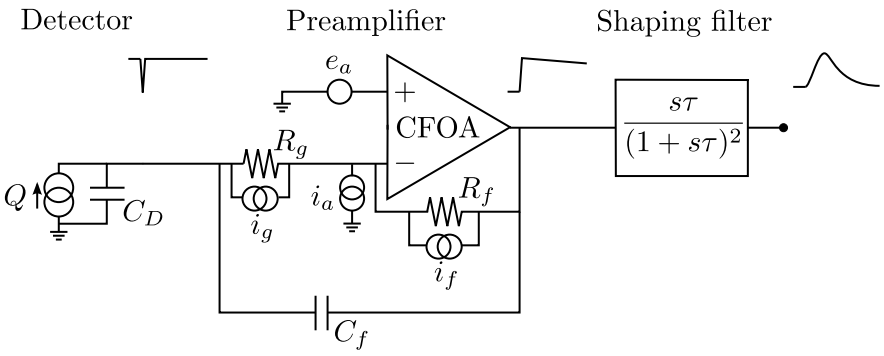

Figure 15. The CFOA charge sensitive preamplifier: full read out chain with preamplifier and shaper, including noise sources of the preamplifier.

at frequencies near $1/2\pi\tau$ the charge sensitive preamplifier behaves like an ideal integrator. In all following calculations we will consider the CFOA to be ideal, and since the shaper filters all frequencies far from $1/2\pi\tau$, we can approximate equation 4.13 as

$$V_{\text{out}}(s) = -\frac{R_f}{1+sR_f\,(C_f+C_c)}Q \simeq -\frac{1}{s\,(C_f+C_c)}Q, \tag{6.2}$$

which in time domain becomes a step:

$$V_{\text{out}}(t) \simeq -\frac{Q}{C_f+C_c}\theta\,(t)\,. \tag{6.3}$$

The output voltage pulse of the whole chain in response to a charge Q in $t=0$ is

$$V_{\text{out}}(s) = -\frac{Q}{s(C_f+C_c)}F(s) = -\frac{\tau}{(1+s\tau)^2}\frac{Q}{C_f+C_c}, \tag{6.4}$$

which in time domain becomes

$$V_{\text{out}}(t) = -\frac{Q}{C_f+C_c}\frac{t}{\tau}\exp\left(-\frac{t}{\tau}\right)\theta(t). \tag{6.5}$$

The read out chain comprised of the preamplifier and the ideal shaper is depicted in figure 15, which shows also the main noise sources in the preamplifier: the CFOA itself, with its voltage and current contributions $e_a(s)$ and $i_a(s)$, and the thermal contributions of resistors R_g and R_f, modeled as current generators $i_g(s)$ and $i_f(s)$. Since we are dealing with high frequency applications, we assume all the low frequency (flicker) noise contributions to be negligible, and all noise generators to have a constant power spectral density.

In the first place, let us calculate the voltage at the output due to the noise sources, one at a time. From the node equations, and with the same approximations on Z_{OL} that led to equation 4.13, it can be shown that the noise due to R_g gives at the output of preamplifier

$$V_{i_g}(s) = \frac{s(C_D+C_f)R_gR_f}{1+s(C_f+C_c)R_f}i_g(s) \simeq \frac{C_D+C_f}{C_f+C_c}R_g i_g(s), \tag{6.6}$$

while noise from R_f gives

$$V_{i_f}(s) = \frac{(1+s(C_D+C_f)R_g)R_f}{s(C_f+C_c)R_f}i_f(s) \simeq \frac{1}{s(C_f+C_c)}i_f(s). \tag{6.7}$$

2011 JINST 6 P05004

Current noise from the amplifier has the same transfer function as $i_f(s)$, so it is given by

$$V_{i_a}(s) \simeq \frac{1}{s(C_f + C_c)} i_a(s). \tag{6.8}$$

and finally for the voltage noise of the amplifier

$$V_{e_a}(s) = \frac{1 + s(C_D + C_f)(R_g + R_f)}{(C_f + C_c)R_f} e_a \simeq \frac{C_D + C_f}{C_f + C_c} e_a. \tag{6.9}$$

It is clear that e_a and $R_g i_g \equiv e_g$ share the same transfer function: R_g gives a voltage or "series" noise contribution, like e_a, while R_f gives a current or "parallel" noise contribution, like i_a.

The noise at the output of the full chain due to each contribution is given by the above expressions multiplied by the shaper transfer function $F(s)$:

$$V_{\text{series}}(s) = \frac{C_D + C_f}{C_f + C_c} F(s) e_{\text{series}}(s) \tag{6.10}$$

for the series noise contributions, and

$$V_{\text{parallel}}(s) = \frac{F(s)}{s(C_f + C_c)} i_{\text{parallel}}(s) \tag{6.11}$$

for the parallel noise contributions. To obtain the squared r.m.s. output noise, one must put $s = i\omega$ in the above expressions, take the mean squared amplitude, and integrate over frequency. For the series noise,

$$|V_{\text{series}}|^2 = \left(\frac{C_D + C_f}{C_f + C_c}\right)^2 |\overline{e_a}|^2 \frac{1}{2\pi} \int_0^\infty d\omega \, |F(i\omega)|^2, \tag{6.12}$$

and since

$$\frac{1}{2\pi} \int_0^\infty d\omega \, |F(i\omega)|^2 = \frac{1}{2\pi} \int_0^\infty d\omega \frac{\omega^2 \tau^2}{(1 + \omega^2 \tau^2)^2} = \frac{1}{8\tau} \tag{6.13}$$

the series output noise becomes

$$|V_{\text{series}}|^2 = \left(\frac{C_D + C_f}{C_f + C_c}\right)^2 \frac{|\overline{e_a}|^2}{8\tau}, \tag{6.14}$$

giving thus a contribution which is inversely proportional on the shaping time. On the other side, for the parallel noise,

$$\left|V_{\text{parallel}}\right|^2 = \left(\frac{1}{C_f + C_c}\right)^2 |\overline{i_a}|^2 \frac{1}{2\pi} \int_0^\infty d\omega \left|\frac{F(i\omega)}{i\omega}\right|^2, \tag{6.15}$$

and since

$$\frac{1}{2\pi} \int_0^\infty d\omega \left|\frac{F(i\omega)}{i\omega}\right|^2 = \frac{\tau^2}{2\pi} \int_0^\infty d\omega \frac{1}{(1 + \omega^2 \tau^2)^2} = \frac{\tau}{8} \tag{6.16}$$

the parallel output noise becomes

$$\left|V_{\text{parallel}}\right|^2 = \left(\frac{1}{C_f + C_c}\right)^2 \frac{\tau |\overline{i_a}|^2}{8}, \tag{6.17}$$

2011 JINST 6 P05004

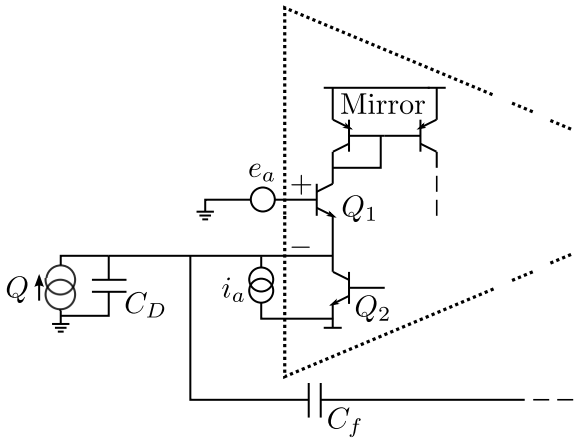

Figure 16. A basic CFOA circuit: current noise from Q1 can be modeled as a voltage noise in series with the base of Q1 (as common practice), i.e. at the non-inverting input, while current noise from the polarization transistor Q2 is a current source at the inverting input. Other noise sources from transistors inside the CFOA were neglected.

giving a contribution which is directly proportional to the shaping time. All the contributions must be added together in quadrature to give a total output noise

$$|V_{\text{tot}}|^2 = |V_{\text{series}}|^2 + |V_{\text{parallel}}|^2 = \left(\frac{1}{C_f + C_c}\right)^2 \left(\frac{\tau}{8}\left(|\overline{i_a}|^2 + |\overline{i_f}|^2\right) + \frac{(C_D + C_f)^2}{8\tau}\left(|\overline{e_a}|^2 + |\overline{e_g}|^2\right)\right). \tag{6.18}$$

We can now calculate the equivalent noise charge by dividing the output noise voltage by the gain from input to output. The gain for a charge Q at the output of the preamplifier is given by equation 6.5, whose peak value is $Q/e(C_f + C_c)$, where $e \simeq 2.72$ is Euler's number. The ENC is thus given by

$$ENC = e(C_f + C_c)\,|V_{\text{tot}}| = \frac{e}{2\sqrt{2}}\sqrt{\tau\left(|\overline{i_a}|^2 + |\overline{i_f}|^2\right) + \frac{(C_D + C_f)^2}{\tau}\left(|\overline{e_a}|^2 + |\overline{e_g}|^2\right)}. \tag{6.19}$$

This quantity must be compared with the charge Q from the detector, and should be at least a factor of 10 or 20 below Q for a decent signal to noise ratio.

If the integrator time constant cannot be considered much bigger than the filter time constant, i.e. if $\tau \simeq (C_f + C_c)(R_f||R_c)$, the calculations are a bit more complicated, and the effect is similar to that of a CR^2-RC shaping filter. If this is the case, the coefficients in equation 6.19 should be modified accordingly, leading to a slightly higher noise charge.

Let us now evaluate the ENC for a typical configuration with $C_D = C_F = 3$ pF, $R_F = 20$ kΩ, $R_g = 500\ \Omega$, for a OPA695 from Texas Instruments. The parallel noise of R_f is given by $\left|i_f\right|^2 = 4k_BT/R_f \simeq 1\ \text{pA}/\sqrt{Hz}$ (where k_B is the Boltzmann constant, and T is temperature, which we assume to be 300 K). The series noise of R_g is given by $|e_g|^2 = 4k_BTR_g \simeq 3\ \text{nV}/\sqrt{Hz}$. From the OPA695 datasheet we find the series noise of the opamp to be $|e_a| \simeq 1.7\ \text{nV}/\sqrt{Hz}$ and its current noise at the inverting input to be $|i_a| \simeq 22\ \text{pA}/\sqrt{Hz}$. The overall noise is largely dominated by this last contribution. With a short shaping time of $\tau = 5$ ns, to minimize the weight of the current noise and to exploit the wide bandwidth of the CFOA, the equivalent noise charge given

2011 JINST 6 P05004

by equation 6.19 is about 6 ke$^-$ r.m.s., dominated by $|i_a|$. This yields a f.w.h.m. noise of about 15 ke$^-$. On the other side, the contribution of the series noise is less than 1 ke$^-$ r.m.s., always quite negligible when compared to the parallel part, unless the detector has a very large capacitance. A longer shaping time worsens things a bit, since the parallel part of the ENC is proportional to $\sqrt{\tau}$, and would possibly make the use of a CFOA not preferable compared to the slower but less noisy VFOA-based configuration.

Even if the exact values depend on the specific CFOA model, we found all CFOAs to have about the same current noise at the inverting input, about 20 pA$/\sqrt{Hz}$. This is the main limit on the noise performances of this configuration, and makes it useful to read out charges of only about 100 ke$^-$ or more. The reason for this lies in the fact that the negative input of the CFOA is canonically connected to the emitter or source of the transistors of the input stage. Figure 16 shows a basic CFOA circuit: it can be seen that the input signal at the inverting node has to be directly compared to the shot noise from the current source for the input transistor. This current can be as high as 1 mA for high frequency operation, giving $|i_a| \simeq 20$ pA$/\sqrt{Hz}$ of shot noise. Thus, this configuration will provide an adequate signal to noise ratio only in case of high energy radiation or in case the detector is some sort of photomultiplier (where a charge of the order of 1 Me$^-$ is expected). Unfortunately, it will not fit the noise requirements of other kinds of detectors which yield smaller charge signals.

References

[1] S. Franco, *Current-feedback amplifiers*, in *Analog circuit design: art, science and personalities*, J. Williams ed., Butterworth Heinemann, U.S.A. (1991), chapter 25.

[2] National Semiconductor, *Current-feedback myths debunked*, OA-20 (1992).

[3] National Semiconductor, *Current feedback amplifiers*, OA-31 (1992).

[4] G. Palumbo and S. Pennisi, *Current-feedback amplifiers versus voltage operational amplifiers*, *IEEE Trans. Circuits Syst.* **48** (2001) 617.

[5] S. Franco, *Design with operational amplifiers and analog integrated circuits*, McGraw-Hill, U.S.A. (2002), see pages 347-397.

[6] National Semiconductors, *Current feedback op amp applications circuit guide*, OA-07 (1988).

[7] J. Mahattanakul and C. Toumazou, *A theoretical study of the stability of high frequency current feedback op-amp integrators*, *IEEE Trans. Circuits Syst.* **43** (1996) 2.

[8] B. Maundy, S.J.G. Gift and P.B. Aronhime, *A novel differential high-frequency CFA integrator*, *IEEE Trans. Circuits Syst. II* **51** (2004) 289.

[9] E. Gatti and P. Manfredi, *Processing the signals from solid-state detectors in elementary-particle physics*, *Nuovo Cim.* **9** (1986) 1.

[10] V. Radeka, *Low-noise techniques in detectors*, *Ann. Rev. Nucl. Part. Sci.* **38** (1988) 217.

2011 JINST 6 P05004